Hasan Kaya* and Mehmet Uçar

Fatigue Behaviour and Mechanical Properties of ECAP'ed and Thixoformed AA7075

Abstract: In this study, the effects of thixoforming, both equal channel angular pressing (ECAP) and thixoforming on high cycle fatigue and fatigue surface morphology of AA7075 have been examined. Experiments are carried out with the same sample materials (AA7075) at a constant temperature (483 K) and the "C" route for 4 passes at ECAP process. In the process of thixoforming is 20 min at 888 K for waiting and 1 min at 673 K for pressing implemented. 140 MPa, 120 MPa and 100 MPa strength values were used at fatigue tests. The microstructural characterizations of the samples were carried out by using optical microscope (OM), scanning electron microscope (SEM) and transmission electron microscope (TEM). This study is an attempt in detail to transformation fine and spherical grain structure with thixoforming process of minimized grain structure by ECAP. As a result of this study, it was seen that ECAP (1 pass) + semi-solid processing (SSP) applied samples have the highest hardness value (171 HV). When the values that are obtained after fatigue strength analyzed, SSP applied materials' property gave the best results and ECAP (1 pass) + SSP applied samples' results were second. When the both process applied materials' optimum values are investigated, it was observed that ECAP 1 pass + SSP applied material is more appropriate in terms of high hardness and fatigue life.

Keywords: equal channel angular pressing, thixoforming, AA7075, fatigue behavior, mechanical properties, microstructures

***Corresponding author: Hasan Kaya:** Department of Machine and Metal Technology, Vocational School of Asim Kocabiyik, Kocaeli University, Kocaeli 41800, Turkey.
E-mail: hasan.kaya@kocaeli.edu.tr
Mehmet Uçar: Department of Automotive Engineering, Technology Faculty, Kocaeli University, Kocaeli 41380, Turkey

1 Introduction

Nowadays, Al alloys are used in many areas of industry. Due to the high mechanical properties of Al alloys 7xxx series, it's preferred in automobile and aerospace industry. Recently there have been many studies to improve the mechanical properties of 7xxx series Al alloys [1–7]. One of these studies, enhancing of strength and ductility properties by grain shrinking with severe plastic deformation (SPD) method comes to the fore. Ultra-fine grain (UFG) structure that couldn't be obtained by traditional production methods, but it can be achieved with SPD [8, 9]. SPD processes, such as ECAP is the most effective process to prepare UFG Al alloy to obtain high mechanical properties [10, 11]. It has been determined that ECAP is especially favorable due to its ability to produce UFG materials with multiple compressions, accumulative roll bonding and torsional straining in full dense conditions without changing the cross-sectional dimensions of the samples [12–18]. On the other hand is it possible to obtain significant grain refinement together with dislocation hardening with ECAP [19, 20]. One of the factors that are affecting the mechanical properties of materials is grain structure. Spherical grain structure increases impact strength, strain property and shock absorption capability property of materials. In order to obtain the spherical grain structure, SSP is used. Thixoforming process is also one of the shaping methods with SSP. It was pointed out that semi-solid processing by thixoforming processes refers to the shaping of metals by extrusion at a temperature between solidus and liquids. Thixoforming process is known that for the alloy to be shaped in the semi-solid state it must have a non-dendritic structure [21–25]. Until now, in order to improve the mechanical properties of AA7075's, there have been many studies including ECAP, SSP, ECAP + SSP processes. At these studies mechanical properties of AA7075 were investigated. However, there is no detailed study which investigates fatigue behavior of ECAP + SSP applied AA7075. Therefore, the present study aims to the grain structure, grain size, hardness, fatigue strength and fracture surfaces were examined by AA7075 subjected to ECAP + SSP.

2 Experimental procedure

The AA7075 with the chemical composition of 5.60 Zn, 2.53 Mg, 1.59 Cu, 0.22 Fe, 0.21 Cr, 0.14 Si, 0.11 Mn and Al

balance in the form of extruded ingot with the diameter of 25 mm, used in the present work. The as received Al extruded ingot was machined into small billets and then homogenized at 753 K for 2 h.

At this study, the as-extruded AA7075 alloy was machined into billets for ECAP with diameter of 20 mm and a length of 55 mm. The ECAP die had characteristic angles $\phi = 90^{o}$ and $\psi = 0^{o}$. The ECAP was conducted at 483 K die temperature for 1 pass, 2 pass, 3 pass and 4 pass respectively, using axial route C and stroke speed of 9×10^{-2} m/min. The liquid fraction against temperature curve was estimated by differential scanning calorimetry (DSC). The results show that the semi-solid region is between 754.8 K and 914.8 K. At this study was chosen as working temperature at 888 K in 20 min and as die temperature at 673 K in 1 min. After ECAP'ed AA7075 billets were cylindrical samples with 15 mm in diameter and 55 mm height, machined from the extruded bar. These dimensions were chosen to obtain a complete filling of the die after thixoforming process.

This process was carried out on the hydraulic 120 kN press and stroke speed of 12×10^{-2} m/min. After heating and forming, the set were samples quenched. MoS_2 is using to lubricate in the process. The temperature of the slug was monitored by a K-type thermocouple embedded in the slug. After the required temperature was reached, the thermocouple was removed and the heated slug raised and compressed into the die at a constant ram speed.

Vicker's micro hardness and fatigue tests were performed to determine the mechanical properties of the ECAP'ed and semi-solid processed AA7075. The samples for fatigue testing were machined along longitudinal axis of the supplied extruded ingot for the bulk AA7075, according to ASTM E606/E606-12. The sample dimensions are shown in Fig. 1. Prior to testing, in order to minimize the introduction of residual stresses throughout the machining operation of the samples, they were polished.

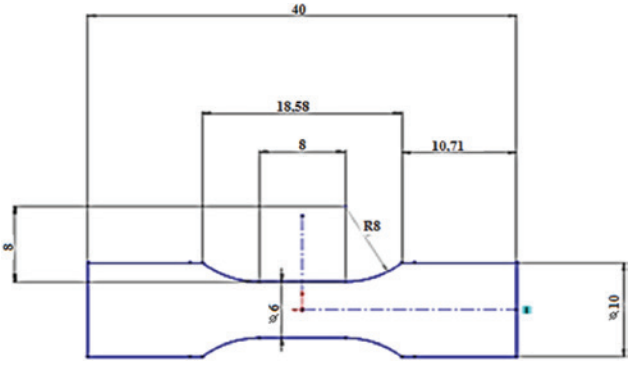

Fig. 1: Dimensional details of high cycle fatigue sample

Fatigue tests were carried out on the four point bending fatigue test machine.

3 Results and discussion

3.1 Microstructure characterization

The OM images, SEM images and TEM images of the ECAP'ed and thixoformed AA7075 are examined. The OM images are shown in Fig. 2. The microstructure of the thixoformed AA7075 exhibits spheroidal grains. Hence the microstructure of the ECAP'ed and thixoformed AA7075 exhibits spheroidal grains lying parallel to the ECAP pass. While the average grain size (ASTM E112 Materials Science Quality Control MSQ analysis program) is around 10.8 for thixoformed samples, the grain size is reduced to ECAP'ed and thixoformed samples. The grain size of samples are 4.8 for ECAP 1 passed and thixoformed, 5.2 for ECAP 2 passed and thixoformed, 5.4 for ECAP 3 passed and thixoformed and 8.3 for ECAP 4 passed and thixoformed.

When the OM images are analyzed which is given in Fig. 2, grain structure of ECAP and thixoformed samples seems smaller than only thixoformed sample microstructure. With the increase in the number of pass ECAP, at ECAP and thixoformed samples, in addition to grain growth globalization of grain structure appears more prominent. In this study thixoformed, ECAP'ed (1 pass, 2 pass, 3 pass and 4 pass) and thixoformed of AA7075 sample's SEM images and EDS (Electron Diffraction Spectrometry) analyze images were given (Fig. 3 and Fig. 4). When the thixoformed sample's SEM images are analyzed, spheroidal grain structure of microstructure image can be seen more clearly than ECAP'ed and thixoformed samples. However grain sizes of ECAP'ed and thixoformed samples are smaller than only thixoformed sample. That is given in Fig. 3. At the thixoformed sample's microstructure it is not observed there is dentritic structure. It's reason that dendritic arms breaking into smaller grain structure. Also, these grains transforms into a spheroidal morphology with applying pressing presure, temperature and holding time in the thixoform die.

When the SEM images of samples applied ECAP and thixoformed at various passes, analyzed (Fig. 4), it seems that microstructure images are made of spherical particles. Samples' small and spherical grain structure at first pass numbers, changes to smaller size spherical grains with the increase of pass numbers. Even if samples applied ECAP and thixoformed have bigger and spherical structure, when look carefully spherical structure

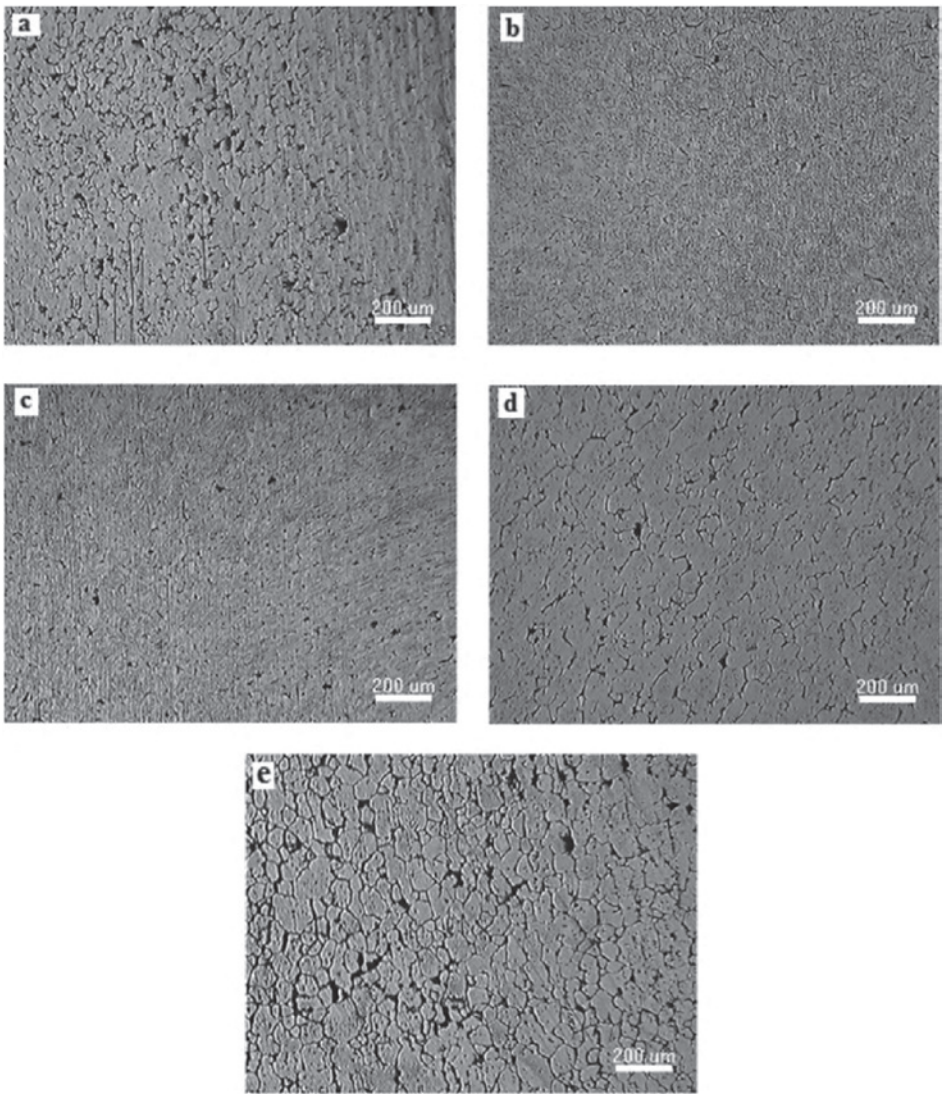

Fig. 2: Optical micrograph of AA7075; ECAP 1 passed + Thixoformed (a), ECAP 2 passed + Thixoformed (b), ECAP 3 passed + Thixoformed (c), ECAP 4 passed + Thixoformed (d), Thixoformed (e)

samples' arrangement has a certain direction and they are being ellipse towards that direction. Also taken EDS images give information about AA7075 materials chemical composition and places where the majority of elements are in the microstructure with high amounts of Mg, Zn and Cu elements can be found freguently. The specified elements are shown with EDS analysis taken from one or two points.

Grain sizes for the ECAP process applied samples can be reduced up to nano level. At this study, after OM and SEM application, TEM studies were applied in order to see microstructure more clearly and obtain detailed information about grain sizes and shapes. The TEM images of ECAP'ed (1 pass, 2 pass and 4 pass) and thixoformed AA7075 samples are shown in Fig. 5. ECAP'ed and thixoformed samples' grain structures are seen as band shape arrangement. Deformation flow lines and grain boundaries are also seen clearly with the effect of processing temperature. The majority of the microstructure after each passes consists of somewhat elongated regions subdivided by the dislocation boundaries oriented to the ECAP pass direction. These boundaries mostly have low angle disorientation.

At ECAP'ed and thixoformed samples together with the increasing number of passes there has been a reduction in grain sizes and UFG structure was obtained. However, in order to obtain spherical grain structure at ECAP'ed samples were subjected to a heat treatment for thixoforming. In this case decreased grain size at ECAP passes are increasing at thixoforming. When ECAP'ed and

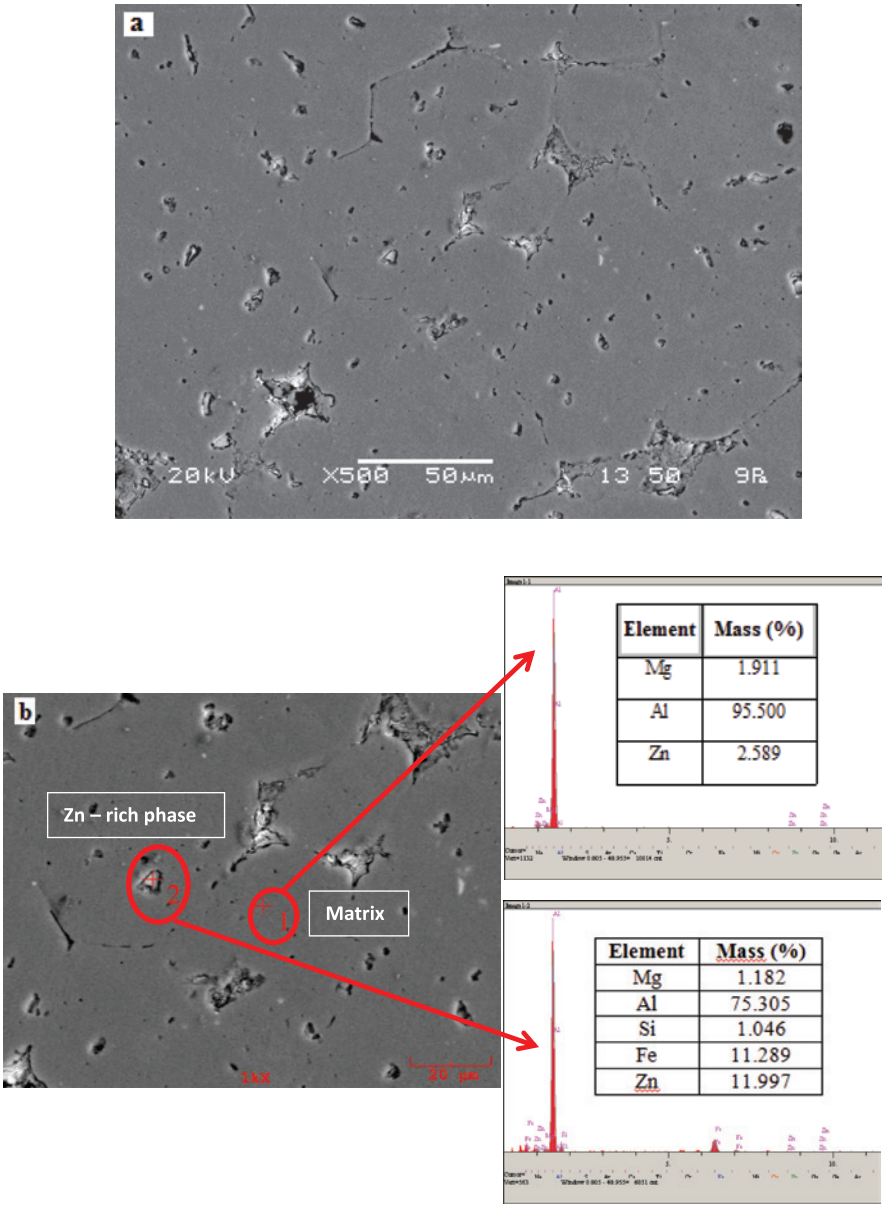

Fig. 3: The SEM Microstructure of the thixoformed AA7075 (a), EDS graphic (b)

thixoformed samples' images analyzed grain structures were directed to one side depending on the direction of pass and there has been a spherical-shape structure.

Together with the deformation processes that are applied to the metals, deformation hardening is occurred. Even if SPD process provides grain size reduction, it also provides decreasing at re-crystallization temperature. However, decreasing re-crystallization temperature causes to occur bigger grain sizes at deformation mechanisms made of lower temperature. Increasing of the grain sizes causes a decrease in strength. TEM analysis shows that $MgZn_2$ precipitate which is rod like structure and seen at AA7075 casting microstructure, distributed throughout the sample by separation smaller spherical particles with ECAP.

3.2 Mechanical properties

An important improvement in mechanical properties of AA7075 alloy obtained after ECAP'ed and thixoformed compared to thixoformed bulk AA7075. Fig. 6 shows the effect of thixoforming and ECAP'ed and Thixoforming over hardness properties of the AA7075. The hardness of the ECAP'ed and thixoformed samples have decreased from 171 HV to 145 HV (nearly 84% decrease) due to the increase

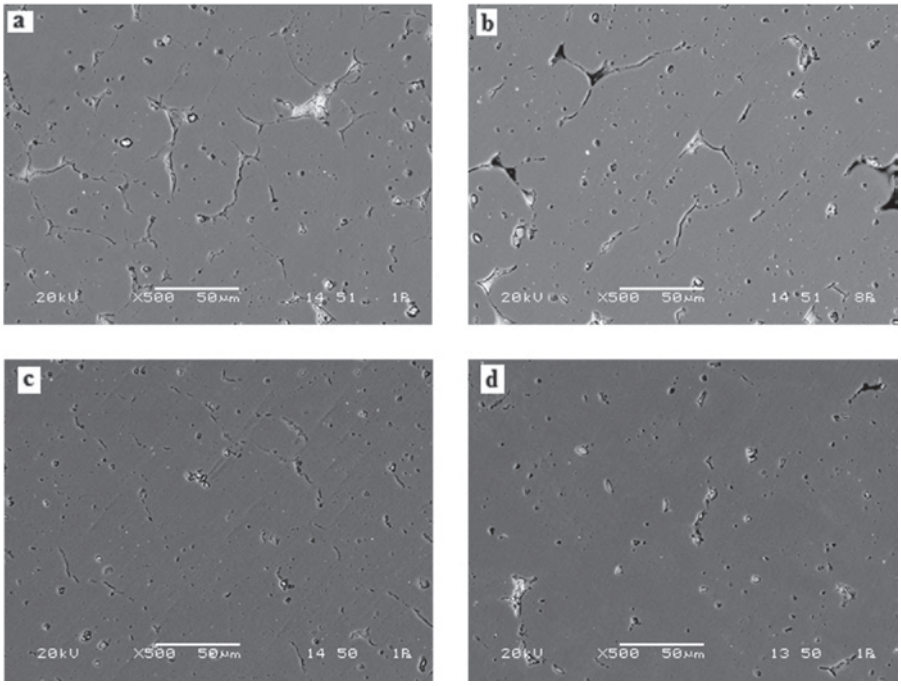

Fig. 4: The SEM Microstructure of the ECAP'ed and thixoformed AA7075; 1 passed (a), 2 passed (b), 3 passed (c) and 4 passed (d)

of pass number. However, the hardness of the just thixoformed sample is 112 HV and this hardness value is increased to 171 HV after ECAP 1 passed processing (nearly 152% increase) as shown in Fig. 6. The hardness data of the AA7075 alloy samples measured after each pass.

As a result of the values only casting process applied samples' hardness value was obtained at the lowest level (97 HV) according to just thixoformed, ECAP'ed and thixoformed samples' values. ECAP'ed and thixoformed samples' measured hardness values were shown decrease with the increase of the pass number and the highest hardness value (171 HV) were obtained at 1 pass applied sample. Thixoformed samples' average hardness value was measured as 112 HV. Pass numbers' effect to hardness of materials was investigated with the ECAP studies that are made on variety of materials. Obtained results show variability according to ECAP process applied materials. While the highest hardness value was reached at 4 passes, next times after these passes there has been a decrease at hardness values [26–29]. That's reason arise from deterioration and recovery in materials crystal structure. Dislocations occurred because of severe plastic deformation (SPD) act as a lock and provide a compacting between atoms and create an increase at hardness. The reason of measured hardness values' increasing is dislocation density and grain thinning which are occurred because of breaking up precipitation [10, 26, 30–32].

3.3 High cycle fatigue properties

Thixoformed, ECAP 1 Passed + Thixoformed, ECAP 2 Passed + Thixoformed, ECAP 3 Passed + Thixoformed and ECAP 4 Passed + Thixoformed AA7075 samples are tested to four point bending fatigue test equipment. The graph of the results is given in Fig. 7.

Figure 7 shows the stress versus number of cycles to failure curve for the thixoformed, ECAP'ed and thixoformed AA7075. It is observed that at an alternating stress level of 140 MPa, the number of cycles to failure is 5.5×10^7; whereas, at alternating stress of 120 MPa, the number of cycles to failure is increased to 5.9×10^7; whereas, at alternating stress of 100 MPa, the number of cycles to failure is increased to 6.2×10^7 for thixoforming AA7075. On the other hand, for ECAP 1 pass and thixoformed AA7075 sample at stress level of 140 MPa, the number of cycles to failure is 4.6×10^7; whereas at 120 MPa it undergoes 4.8×10^7 cycles to failure and whereas at 100 MPa it undergoes 5.1×10^7 cycles to failure. Also for ECAP 2 pass and thixoformed AA7075 sample at stress level of 140 MPa, the number of cycles to failure is 4.4×10^7; whereas at 120 MPa it undergoes 4.6×10^7 cycles to failure and whereas at 100 MPa it undergoes 4.8×10^7 cycles to failure. On the other hand, for ECAP 3 pass and thixoformed AA7075 sample at stress level of 140 MPa, the number of cycles to failure is 3.9×10^7; whereas at 120 MPa

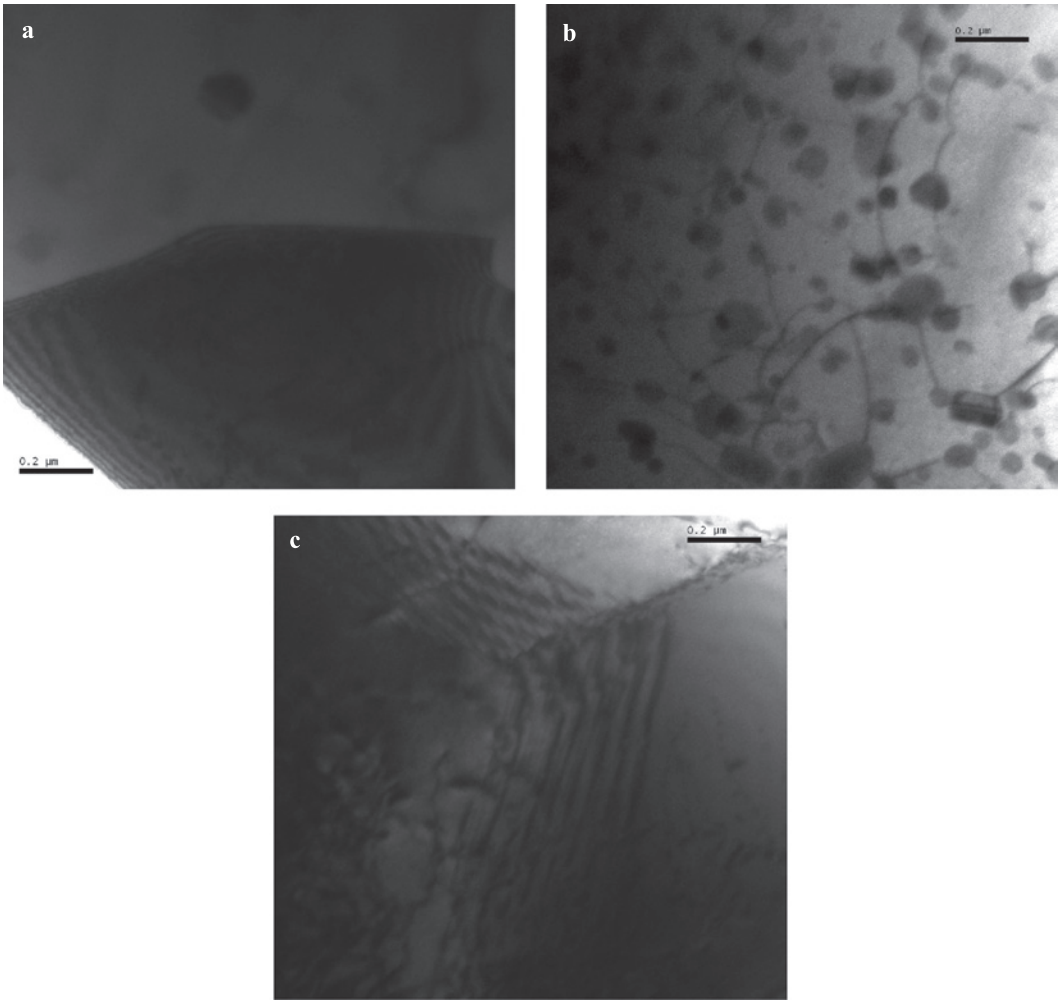

Fig. 5: The TEM Microstructure of the ECAP'ed and thixoformed AA7075; 1 passed (a), 2 passed (b), 4 passed (c)

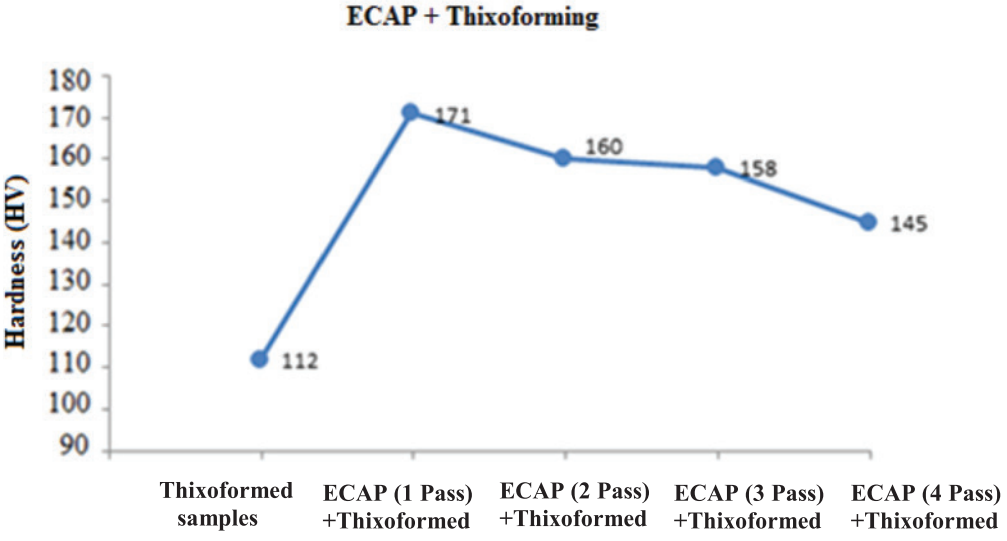

Fig. 6: Vickers hardness of thixoformed, ECAP'ed and thixoformed AA7075 samples

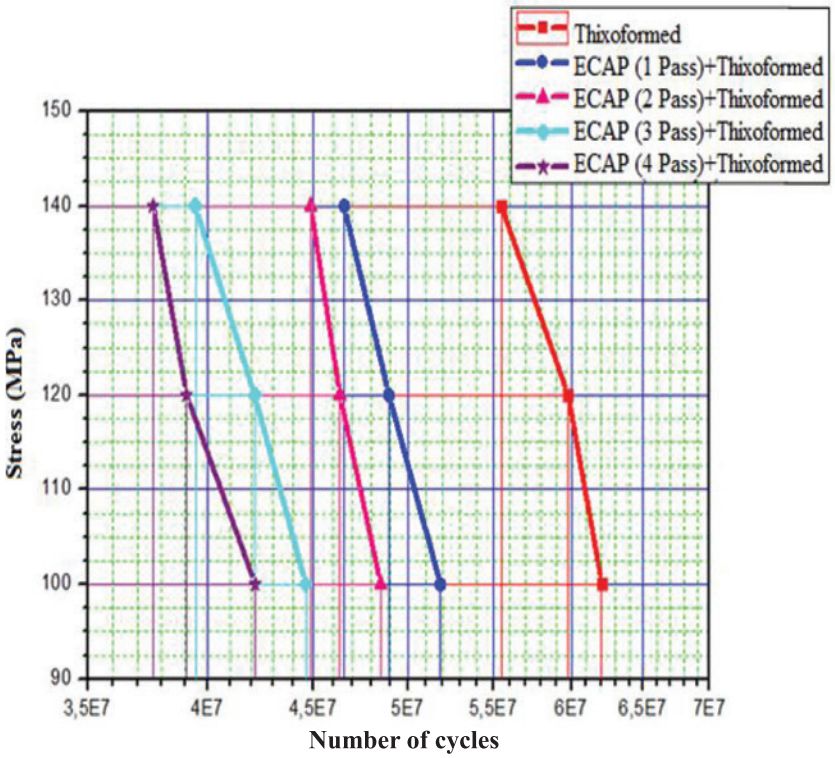

Fig. 7: Comparative S-N curve of Thixoformed, ECAP 1 Pass + Thixoformed, ECAP 2 Pass + Thixoformed, ECAP 3 Pass + Thixoformed, ECAP 4 Pass + Thixoformed of AA7075 samples

it undergoes 4.2×10^7 cycles to failure and whereas at 100 MPa it undergoes 4.4×10^7 cycles to failure. Finally, for ECAP 4 pass and thixoformed AA7075 sample at stress level of 140 MPa, the number of cycles to failure is 3.7×10^7; whereas at 120 MPa it undergoes 3.9×10^7 cycles to failure and whereas at 100 MPa it undergoes 4.2×10^7 cycles to failure.

3.4 Fatigue fracture surface morphology

The fracture surface morphologies of thixoformed samples, ECAP'ed and thixoformed samples' have been investigated under SEM images are given in Fig. 8 and Fig. 9. Shapes of grain structures which are changed spherical structure are seen at thixoformed samples' fracture surfaces. It's observed that the dimple size which is cause to fatigue fracture at only thixoform applied sample is bigger than ECAP and thixoform applied samples. The reason of grain growth is no application of ECAP primary deformation process and so can't provide decrescent. The reason of the increasing at ECAP and thixoform applied samples' grain size is application of thixoform after ECAP. However, as seen on SEM images of fatigue fracture

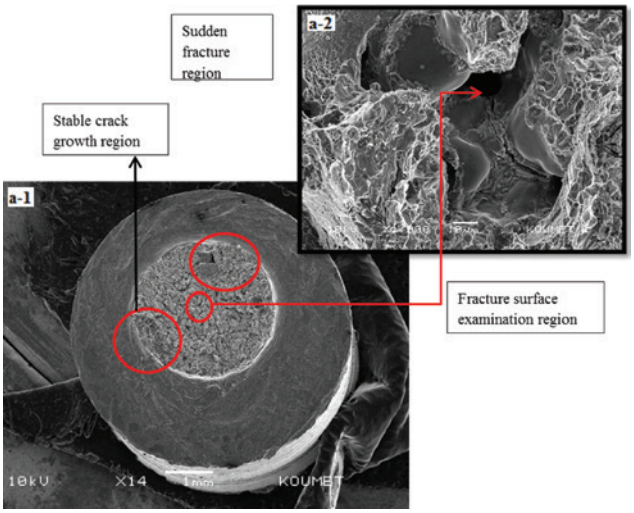

Fig. 8: The SEM image of fracture surface morphology of thixoformed AA7075 after high cycle fatigue test

analyze, spherical grain structure is obtained at thixoformed samples.

It's seen that grain structures are in spherical morphology, especially after fracture surface analyze at just thixoformed, ECAP'ed and thixoformed samples.

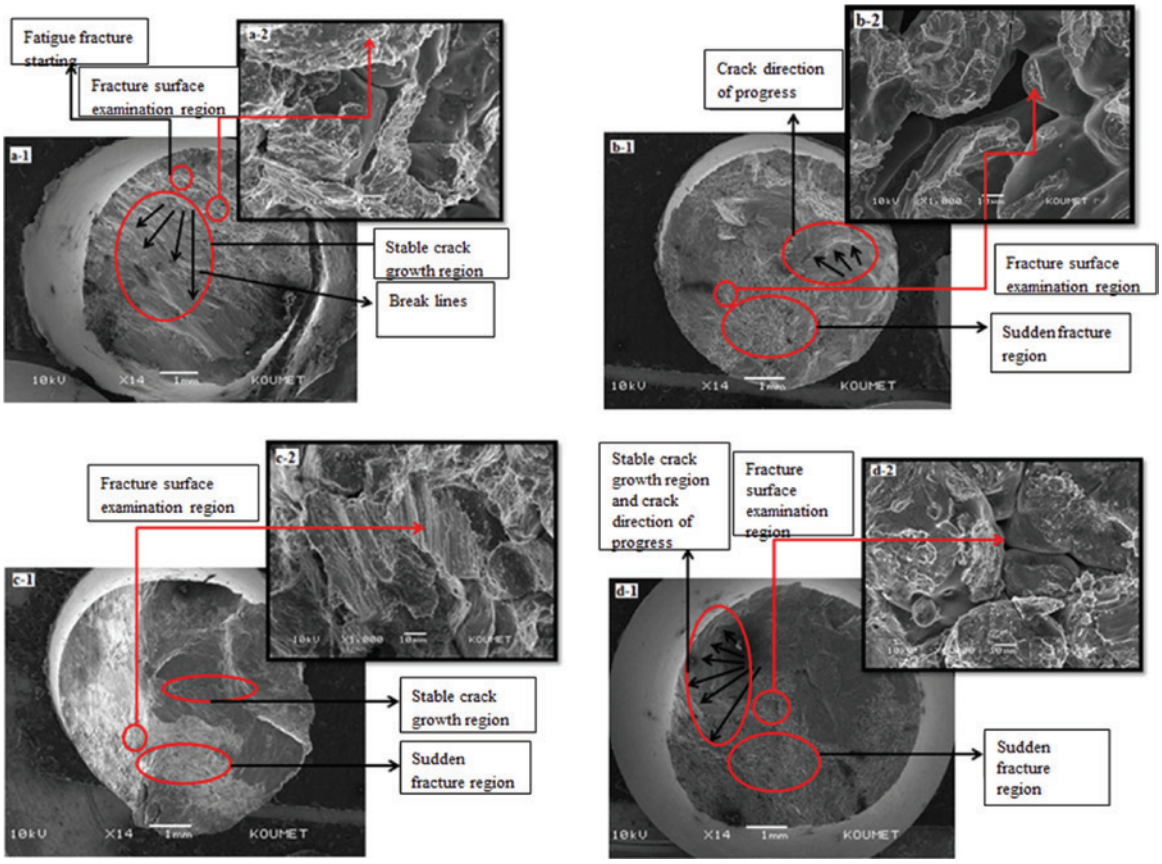

Fig. 9: SEM images of fracture surface morphology of ECAP'ed and thixoformed AA7075 after high cycle fatigue test; 1 passed (a1–a2), 2 passed (b1–b2), 3 passed (c1–c2), and 4 passed (d1–d2)

Spherical grain structure is mostly resulted sudden fracture regions' and stable crack regions' majority at fatigue fractures. Its reason can be explain spherical grain structure's easily take out from grain boundaries at the regions which the crack starting is occurred while fatigue stress. At ECAP 1 pass and thixoformed sample (Fig. 9, a1–a2), it can be seen a structure which has fatigue crack starts, directions, break lines and crack advance region. At ECAP 2 pass and thixoformed sample (Fig. 9, b1–b2), it can be seen crack advance directions and sudden fracture region. At ECAP 3 pass and thixoformed (Fig. 9, c1–c2) and at ECAP 4 pass and thixoformed (Fig. 9, d1–d2) samples, it can be seen stable crack advance region and sudden fractures. Sudden fractures are increasing with ECAP pass number in comparison with just thixoformed, ECAP 1 Pass and thixoformed sample. The reason of that increasing is related with SPD rate which is created in material. Together with the increase in the number of deformation, recrystallization temperature is decreased. This decreasing causes growth at grain structure of material and decrease at strength of material [20].

4 Conclusion

In this study, the experimental characterization of high cycle fatigue properties and fracture surface morphology of AA 7075 produced by just thixoforming and by ECAP and thixoforming processes have been examined and the following results were gained.

- After samples' grain sizes are thinned with ECAP, spherical shape is obtained by thixoforming process. However grain sizes are grown. This growth is 40–50% smaller than just thixoformed samples.
- Decreasing was seen at samples' hardness values with increasing number of SPD process. The best hardness value 171 HV was seen at ECAP'ed 1 pass and thixoformed sample.
- Even if fatigue analysis at just thixoformed sample are seen better (5.5×10^7 for 140 MPa, 5.9×10^7 for 120 MPa, 6.2×10^7 for 100 MPa for thixoforming AA7075), when hardness and fatigue strength (4.6×10^7 for 140 MPa, 4.8×10^7 for 120 MPa, 5.1×10^7 for 100 MPa for ECAP 1 pass and thixoformed AA7075 sample) evaluate to-

gether it's clearly seen that ECAP'ed 1 pass and thixoformed samples give the best results.

This study was supported by Kocaeli University Scientific Research Project Unit, with Project Studies nos. 2010/076–2010/058.

Received: July 31, 2013. Accepted: August 23, 2013.

References

[1] P. Das, R. Jayaganthan, T. Chowdhury and I.V. Singh, *Mater. Sci. Eng. A*, **528**, 7124–7132 (2011).
[2] J. Li, Z. Peng, C. Li, Z. Jia, W. Chen and Z. Zheng, *T. Nonferr. Metal Soc.*, **18**, 755–762 (2008).
[3] J.C. Williams and E.A. Starke, *Acta Mater.*, **51**, 5775–5799 (2003).
[4] S.K. Panigrahi and R. Jayaganthan, *J. Alloy Compd.*, **509**, 9609–9616 (2011).
[5] L.J. Zheng, H.X. Li, M.F. Hashmi, C.Q. Chen, Y. Zhang and M.G. Zeng, *J. Mater. Process. Tech.*, **171**, 100–107 (2006).
[6] W.J. Kim, J.K. Kim, H.K. Kim, J.W. Park and Y.H. Jeong, *J. Alloy Compd.*, **450**, 222–228 (2008).
[7] Y.H. Zhao, X.Z. Liao, Z. Jin, R.Z. Valiev and Y.T. Zhu, *Acta Mater.*, **52**, 4589–4599 (2004).
[8] R.Z. Valiev, R.K. Islamgaliev and I.V. Alexandrov, *Prog. Mater. Sci.*, **45**, 103–189 (2000).
[9] Z.C. Wang and P.B. Prangnell, *Mater. Sci. Eng. A*, **328**, 87–97 (2002).
[10] R. Z. Valiev and T.G. Langdon, *Prog. Mater. Sci.*, **51**, 881–981 (2006).
[11] M.Y. Zheng, S.W. Xu, X.G. Qiao, K. Wu, S. Kamado and Y. Kojima, *Mater. Sci. Eng. A*, **483–484**, 564–567 (2008).
[12] Y. Iwahashi and Z. Horita, *Acta Mater.*, **46**, 3317–3331 (1998).
[13] Z. Horita and T. Fujinami, *Metall. Mater. Trans. A*, **31**, 691–701 (2000).
[14] S.L. Semiatin, P.B. Berbon and T.G. Langdon, *Scripta Mater.*, **44**, 135–140 (2001).
[15] Y.T. Zhu and T.C. Lowe, *Mater. Sci. Eng. A*, **291**, 46–53 (2000).
[16] T.G. Langdon, M. Furukawa, M. Nemoto and Z. Horita, *J. Met.*, **52**, 30–33 (2000).
[17] K. Nakashima, Z. Horita and M. Nemoto, *Mater. Sci. Eng. A*, **281**, 82–87 (2000).
[18] A. Yamashita and D. Yamaguchi, *Mater. Sci. Eng. A*, **287**, 100–106 (2000).
[19] L.J. Zheng, C.Q. Chen, T.T. Zhou, P.Y. Liu and M.G. Zeng, *Mater. Charact.*, **49**, 455–461 (2003).
[20] J.K. Kim, H.G. Jeong, S.I. Hong, Y.S. Kim and W.J. Kim, *Scripta Mater.*, **45**, 901–907 (2001).
[21] S. Chayong, H.V. Atkinson and P. Kapranos, *Mater. Sci. Eng. A*, **390**, 3–12 (2005).
[22] H. Guo, X. Yang, J. Wang, B. Hu and G. Zhu, *T. Nonferr. Metal Soc.*, **20**, 355–360 (2010).
[23] A. Neag, V. Favier, R. Bigot and M. Pop, *J. Mater. Process. Tech.*, **212**, 1472–1480 (2012).
[24] D. Özyürek, *Sci. Res. Essays*, **6**, 6222–6226 (2011).
[25] Z. Fan, *Int. Mater. Rev.*, **47**, 137 (2002).
[26] S.R. Kumar, K. Gudimetla, P. Venkatachalam, B. Ravisankar and K. Jayasankar, *Mater. Sci. Eng. A*, **533**, 50–54 (2012).
[27] Y.H. Zhao, X.Z. Liao, Z. Jin, R.Z. Valiev and Y.T. Zhu, *Acta Mater.*, **52**, 4589–4599 (2004).
[28] K.R. Cardosoa, D.N. Travessaa, W.J. Bottac and A.M. Jorge, Jr., *Mater. Sci. Eng. A*, **528**, 5804–5811 (2011).
[29] E.A. El-Danaf, *Mater. Sci. Eng. A*, **487**, 189–200 (2008).
[30] V.M. Segal, *Mater. Sci. Eng. A*, **197**, 157–164 (1995).
[31] H.S. Kim, M.H. Seo and S.I. Hong, *Mater. Sci. Eng. A*, **291**, 86–90 (2000).
[32] M. Furukawa, Z. Horita and T.G. Langdon, *J. Mater. Sci.*, **40**, 909–917 (2005).